THE INFLUENCE OF THE FUSELAGE ON HIGH α VORTICAL FLOWS AND THE SUBSEQUENT EFFECT ON FIN BUFFETING

ICAS-92-7.4.2

A. Vincent and Dr. N. J. Wood

School of Mechanical Engineering
University of Bath
Bath, England

ABSTRACT

An investigation has been undertaken to determine the effect of the fuselage on the fin buffeting characteristics of a generic modern combat aircraft in both the high and low wing configuration. Tests were conducted in the University of Bath 2.1m x 1.5m Low Speed Wind Tunnel utilising a variable configuration, single fin, generic model based on a 60° cropped delta wing planform.

Vortex flowfield unsteady pressure and fin response data was taken to establish a correlation between vortex flowfield excitation and fin response, supported by laser light sheet flow visualisation.

It was found that peak fin buffeting occurred at 40° and 42° angle of attack for the high wing and low wing configurations respectively. Laser light sheet flow visualisation revealed that in both cases peak buffeting occurred when the wing leading edge vortex shear layers impinged upon the fin leading edge and tip. This angle of attack difference is therefore, deemed to be a function of model geometry.

Unsteady pressure measurements taken at the fin surface showed a sharp rise in the level of pressure fluctuations in the region of peak buffeting. However, the unsteady pressure fluctuations continued at a high level in the post peak buffet region whereas the fin response reduced to a relatively low level. Further analysis of the unsteady pressure data showed that although post peak flowfield energy levels were as high or higher than those at the peak buffet condition the flowfield was less organised and the energy content concentrated at low frequencies (<30Hz).

NOTATION

c	Mean Aerodynamic Chord
f	Frequency (Hz)
f_c	Characteristic Frequency
K	Strouhal Number
K_m	Modified Reduced Frequency Parameter
LERX	Leading Edge Root Extension
LEX	Leading Edge Extension
m	Generalised Mass
$\sqrt{n}G(n)$	Buffet Excitation Parameter
q	Dynamic Pressure
S	Fin Area
U_∞	Tunnel Velocity
z	Fin Tip Acceleration
α	Angle of Attack (AoA)
ζ	Total Damping (fraction of critical)

INTRODUCTION

A prevailing requirement for modern combat aircraft is the ability to sustain controlled flight in the very high, post stall, angle of attack regime[1]. Aircraft that possess this capability exhibit enhanced manoeuvrability and agility. A number of current combat aircraft types are able to achieve relatively high α flight by utilizing vortex generating, lift enhancing devices such as wing Leading Edge Root Extensions (LERX); typically the F/A18 Hornet.

However, current combat aircraft types operating in the high α region of the flight envelope have experienced severe empennage buffeting and in particular, buffeting of the vertical fin. This phenomenon has been attributed to the separated vortical flows generated by the L.E.R.X.'s bursting upstream of and impinging upon the vertical fins[2][3].

Further studies carried out on a simple 60° cropped delta wing fitted with a single fin[4] has shown that single fin buffeting is wing stall related, with the single fin having negligible effect on the vortical flow over the wing.

A complete understanding of the fin buffet phenomenon is essential if an effective means of buffet suppression or attenuation is to be found. Current methods of addressing the problem include fin structural reinforcement and the fitting of L.E.X. fences[5]. However, fin structural reinforcement involves a considerable weight penalty and the L.E.X. fence is very position sensitive.

The aims of this investigation are to determine what effect the presence of a fuselage, in particular a long slender forebody, has on the fin buffet characteristics of a 60° cropped delta wing, and to establish a correlation between the fin response and incident vortical flowfields for both the high and low wing configurations.

EXPERIMENTAL APPARATUS AND PROCEDURES

Tests have been conducted in the University of Bath 2.1m x 1.5m low speed ($45ms^{-1}$) wind tunnel facility to investigate the fin buffeting characteristics of a single fin generic model in both a high and a low wing configuration and thus determine the influence of the fuselage on this phenomenon.

Figure 1 shows the arrangement of the high α model support rig which is capable of angle of attack sweeps from 0° to 90° whilst maintaining the model centre of rotation on the tunnel centre-line. The support rig is primarily a cranked pantograph mechanism mounted on its side to take advantage of the long dimension of the tunnel test section. Rig lateral stiffness is achieved with minimum tunnel blockage by the use of 'A' frames. Angle of attack position is controlled either manually or by computer by means of an

electric linear actuator with position feedback via a separate linear displacement transducer. This arrangement results in a position accuracy of 0.1° and negligible pitch deflection under load. By pivoting the model about a point close to the aerodynamic centre, actuation loads and holding torques are minimised and are independent of the model weight.

The generic model for fin buffet research, shown in figures 2 and 3, comprises a rounded square section fuselage, ogive nose cone and 60° cropped delta wing. The wing is essentially a flat plate 0.015m thick with an elliptical leading edge, tapered trailing edge and a span of 0.6m. The elliptical leading edge profile was selected in preference to a sharp leading edge profile in order that comparisons may be made with other fin buffet attenuation studies being undertaken at the University of Bath. As the wing is symmetrical about its chord the model may represent either a high or low wing configuration due to the provision of two fin attachment points on opposite sides of the rear fuselage.

The generic model may be fitted with either a rigid fin, instrumented for unsteady pressure measurement, or a flexible fin to determine fin buffet response.

Fin Designs For Buffet Analysis

Figure 4 shows the design of the rigid fin used to analyze the pressure fluctuation characteristics of the buffet inducing vortical flow fields. The fin was machined from a solid block of aluminium alloy to give a NACA 0006 section. The fin has a 45° leading edge sweep and a span of 0.22m. A pair of unsteady pressure transducers are mounted flush with the fin surface at the intersection of the 80% span and 40% chord lines, one on each side of the fin.

The flexible fin used to measure fin buffet response is shown in figure 5. The fin is comprised of an aluminium alloy fin spar instrumented with two strain gauges, connected in a half bridge circuit, and positioned near the root. In order to ensure that fin buffeting occurred the fin spar was scaled using a reduced frequency parameter (K) of 0.6 based on the wing mean aerodynamic chord, as suggested by Bean[6], where:

$$K = \left(\frac{f\,c}{U_\infty}\right)$$

The fin spar is enclosed within a segmented balsa wood shroud which
provides an aerodynamic fairing and appropriate fin area. The flexible fin has a first bending frequency of 36Hz.

Both fins are rigidly attached to the model by means of a 'T' shaped root that locates in a slot in the rear fuselage and is then secured by retaining screws.

Data Acquisition

Both the fin buffet response data and the flowfield unsteady pressure data were acquired using a commercially available data acquisition package (GLOBAL LAB™ by Data Translation®) and DT2821 data acquisition board (also by Data Translation®) permitting data sampling rates of up to 50KHz.

The fin response data was sampled at a rate of 5KHz over 5 seconds whereas the unsteady pressure data was acquired at a rate of 3KHz per channel over a 3 second period.

Data Reduction

Data reduction was also performed using the wide range of signal conditioning functions available with the Global Lab package.

The flowfield unsteady pressure data obtained using the rigid fin was reduced to unsteady pressure fluctuation levels and non-dimensionalised by the free stream dynamic pressure, q. Further processing of the pressure data produced Power Spectral Density's (PSD's) to determine the frequency content of the buffet inducing flowfields.

All fin buffet traces were reduced to the non-dimensionalised buffet excitation parameter suggested by Mabey[7]:

$$\sqrt{nG(n)} = \frac{2mz}{qS\sqrt{\pi}}\sqrt{\zeta}$$

where m is the generalised mass, z the rms tip acceleration and ζ the total damping (as a fraction of the critical).

PRESENTATION AND DISCUSSION OF RESULTS

All fin buffet response and unsteady pressure data was obtained at a free stream dynamic pressure of 588 Nm^{-2} which corresponds to a wind tunnel velocity of 30 ms^{-1}.

Flexible Fin Response

Figure 6 shows the level of flexible fin buffet response with the model in both the high and low wing configuration. Peak buffeting occurs at angles of attack of 40° and 42° for the high and low wing configurations respectively. In both cases very little fin response was observed from 0° to 30° angle of attack; the response in this region being the result of disorganised flow unsteadiness. For both high and low wing configurations fin buffet onset occurred at 32° with fin response increasing rapidly to the previously mentioned peak values. Post peak buffet levels reduce sharply to approximately 50% of the peak values. Figure 7 shows the strain gauge output signals at the peak buffeting condition for both the high and low wing cases. The signals clearly show the nature of the fin response.

Flow Visualisation

Laser light sheet flow visualisation (figures 8 & 9) showed that in both the high wing and low wing cases peak fin buffeting coincided with the wing leading edge vortex shear layers impinging on the fin leading edge and tip. Due to the slight difference in relative position of the wing and fin in the high and low wing configurations the vortex shear layers impinge upon the fin tip and leading edge 2° later for the low wing case than in the high wing case. The boundary between the port and starboard vortex shear layers was seen to oscillate to either side of the fin as a result of the anti-phase expansion and contraction of the vortices. In the pre-peak buffet region the coherent vortex shear layers are clear of the fin and move inboard with increasing angle of attack. In the post peak region vortex breakdown was apparent from the size and turbulent appearance of the vortices even though the leading edge roundness reduces the severity of the vortex burst.

Flowfield Unsteady Pressures

Figures 10 and 11 show the level of rms unsteady pressure fluctuations, port and starboard, for the model in the high and low wing configurations. It can be seen that, as with the fin response data, low levels of unsteady pressure fluctuation were measured at angles of attack below 30°. The fluctuation levels then increase to a peak in the region of peak buffeting. However, unlike the fin response data, the pressure fluctuation levels do not reduce in the post peak buffeting region; in the high wing case the post buffet peak pressure fluctuation levels actually increase. The most likely cause of the difference in the buffet levels measured by the port and starboard transducers is a slight vortex asymmetry although this was not detected during flow visualisation.

In order to determine the correlation between vortex flowfield excitation and fin response, short periods of pressure signal, at specific angles of attack, were compared. Figure 12 a & b show 200 milliseconds of pressure signal from the port and starboard transducers for the high wing configuration at 40° angle of attack (peak buffeting condition). Deflection of the fin can only arise from a pressure difference across the fin. Therefore, to emphasise the anti-phase relationship between the port and starboard pressure signals a difference signal was generated by considering only the a.c. components and subtracting one from the other (see figure 12c). This treatment of the data had the additional effect of neutralising the response of the transducers to a source of noise associated with the fan blade passing frequency. It can be seen from figure 12, at the high wing peak buffeting condition, that the flow field is ordered and that a strong anti-phase relationship exists between the port and starboard unsteady pressure signals.

Further processing of the difference signal was undertaken to obtain a Power Spectral Density (PSD) and hence the frequency content of the excitation. Figure 13 shows the PSD's of the difference signals for the high wing configuration at 36°, 40° and 58°; representing pre-buffet, peak buffet and post-buffet conditions. It can be seen that just prior to the peak buffet condition, at 36° AoA, the frequency content is generally broad band with a peak frequency at 66Hz. This PSD pattern is continued at the peak buffet condition, but the energy levels are higher and the frequency peak has been shifted slightly to 63.5Hz. In the post peak buffeting region the PSD shows a significantly higher energy level, but it is concentrated at low frequency (<30Hz). However, the PSD of the post-buffet signal would suggest that sufficient flowfield energy exists at the fin first bending frequency to cause a higher level of fin buffeting than was actually measured. However, at the higher angles of attack the vortical flow field is less ordered and the vortex shear layers no longer impinge upon the fin. Therefore the fin response in this region can be attributed to the fin being immersed in the wake of a bluff body.When the post peak buffet levels are compared with similar results obtained for a wing and single fin combination[4] it can be seen that the post peak buffet level is considerably higher in the presence of a fuselage.

When the low wing unsteady pressure data is presented in this way it can be seen from figure 14 that the port and starboard signals also have a strong anti-phase relationship at the peak buffeting condition. Furthermore, the general pattern of the PSD's for the peak buffet and post buffet conditions (see figure 15) are similar to those for the high wing case. There is however, a difference in characteristic frequency associated with the high and low wing peak buffeting conditions. This characteristic frequency may be used to determine a modified reduced frequency parameter, K_m; where c sin α is used as a means of accounting for the effect of angle of attack and collapses the data to a single value.

$$\left(\frac{f_c\, c}{U_\infty}\right)\sin\alpha = K_m$$

Where f_c is the characteristic frequency, c the mean aerodynamic chord and U_∞ the tunnel velocity. This would result in a high wing value of K_m = 0.63, and a low wing value of K_m = 0.60. These values are close to those provided by Bean[7] for wings of almost identical planform but spans of 0.5m and 0.2m having modified frequency parameters of 0.55 and 0.54 respectively.

It is apparent from the excitation and response results obtained that the flexible fin first bending frequency does not coincide with the characteristic excitation frequencies derived for the high and low wing configurations at the peak buffeting condition. This suggests that if the fin were stiffened to achieve a fin first bending frequency equal to the characteristic excitation frequency then maximum levels of fin buffet response would be achieved at the current tunnel running speed. Alternatively the tunnel speed could be reduced until the characteristic excitation frequency matched the existing fin first bending frequency to achieve the same effect. This would confirm that the tuning of aircraft fins such that none of their normal mode frequencies are within the excitation frequency range is impractical due to the range of speeds and angles of attack encompassed by a modern agile combat aircraft's flight envelope.

CONCLUSIONS

Peak buffeting occurs at angles of attack of 40° and 42° for the high and low wing configurations respectively. This slight difference is attributed to the difference in relative position of wing and fin in the high and low wing configurations.

Peak single fin buffeting occurs when the vortex shear layers impinge upon the fin leading edge and tip and is dependent on a strong anti-phase relationship existing between the port and starboard vortices resulting from an oscillation of the vortex boundary shear layers either side of the fin.

Unsteady pressure fluctuation levels follow the same trend as the fin buffet levels up to and including the peak buffet condition for both the high and low wing configurations. However, at higher angles of attack the fin response reduces considerably even though unsteady pressure fluctuation levels remain high. Frequency analysis of the vortical flowfields show that the reduced fin response in this region is due to the flow energy being concentrated at frequencies well below the fin first bending mode and the absence of the periodic shear layer oscillations about the fin.

The frequency content of the vortical flowfields is generally broad-band but does contain a characteristic peak frequency. This frequency reduces as angle of attack is increased.

REFERENCES

1. Skow, A.M. and Erickson, G.E.
"Modern Fighter Aircraft Design for High Angle Of Attack Manoeuvring"
AGARD LS-121, paper No.4, 1982

2. Triplett, W.E.
"Pressure Measurements on Twin Vertical Tails In Buffeting Flow"
AIAA Paper 82-0641

3. Lee, B.H.K. and Brown, D.
"Wind Tunnel Investigation and Flight Tests of Tail Buffet on the CF-18 Aircraft"
AGARD CP-483, April 1990

4. Bean, D.E. and Wood, N.J.
"An Experimental Investigation of Empennage Buffeting"
AIAA Paper 91-3224

5. Lee, B.H.K. and Brown, D.
"Wind Tunnel Studies of F/A18 Tail Buffet"
AIAA Paper 90-1432

6. Bean, D.E.
University of Bath
Unpublished Data

7. Mabey, D.G.
"Some Aspects of Aircraft Dynamic Loads Due to Flow Separation"
AGARD R-750 (1988)

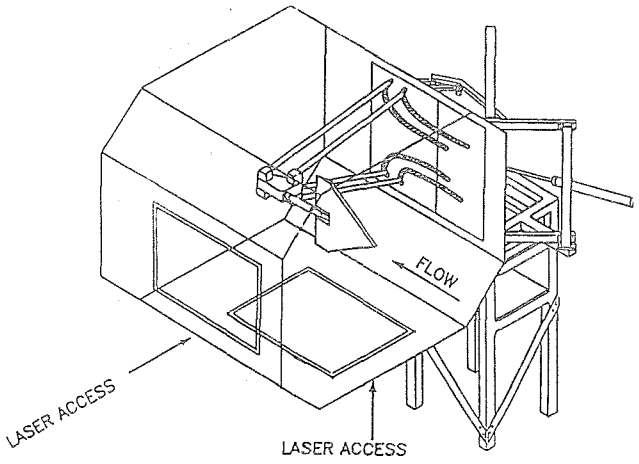

Figure 1: 2.1m x 1.5m Low Speed Wind Tunnel And High α Support Rig.

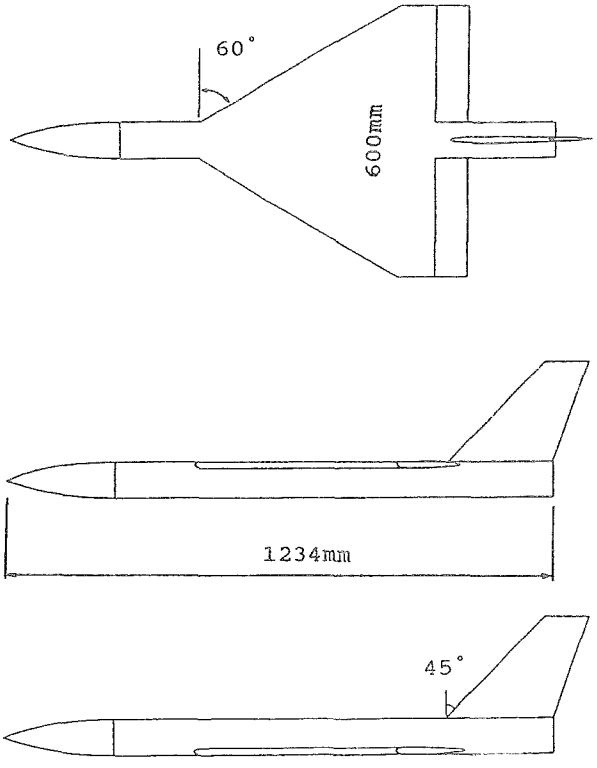

Figure 2: Generic Model For Fin Buffet Research:
a) Plan View.
b) High Wing Configuration.
c) Low Wing Configuration.

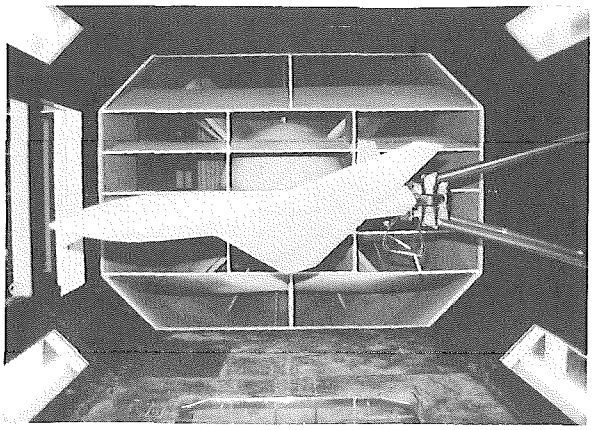

Figure 3: Generic Model For Fin Buffet Research Mounted On High α Rig In 2.1m x 1.5m Wind Tunnel.

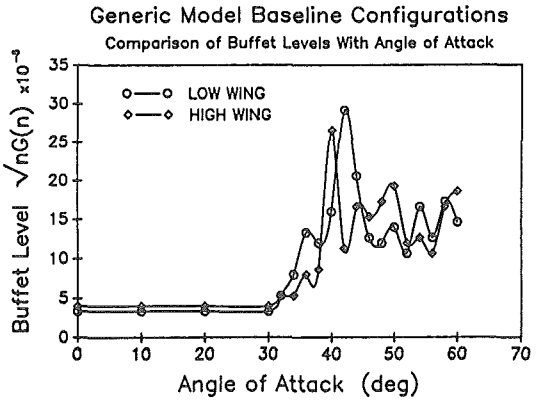

Figure 6: Fin Buffet Response.

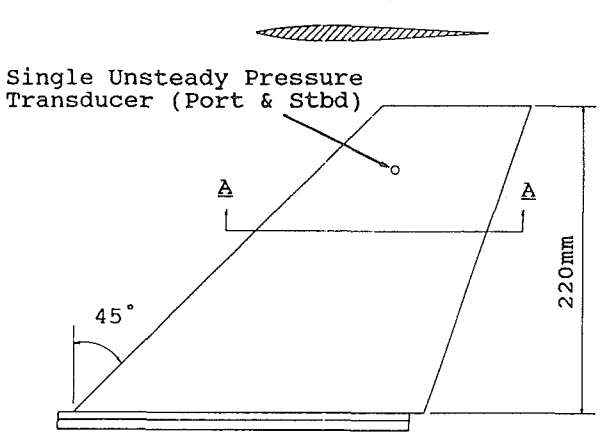

Figure 4: Rigid Fin Design.

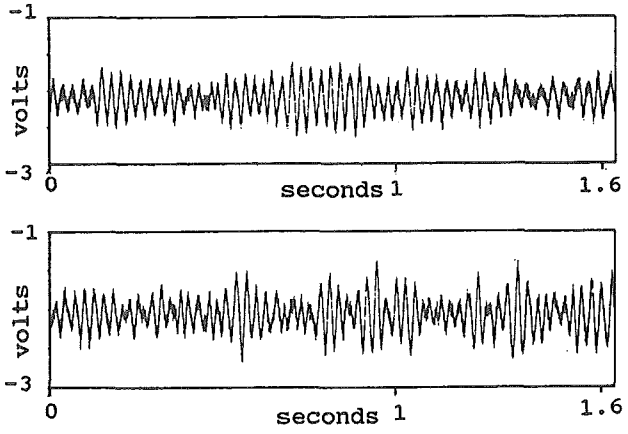

Figure 7: Peak Buffeting Strain Gauge Output Signals:
a) High wing configuration at α=40°
b) Low wing configuration at α=42°

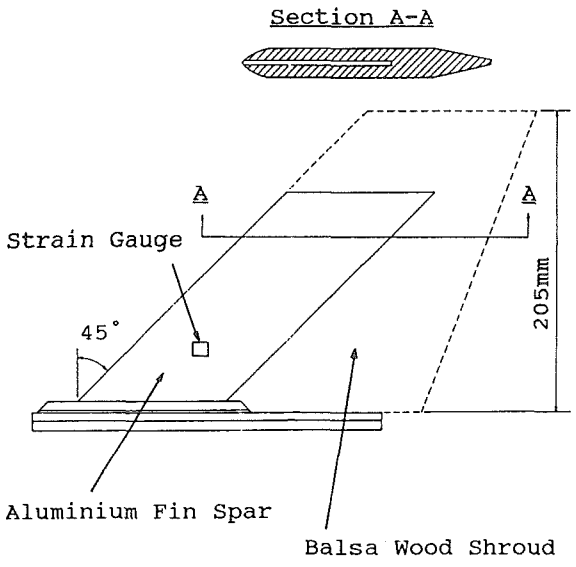

Figure 5: Flexible Fin Design.

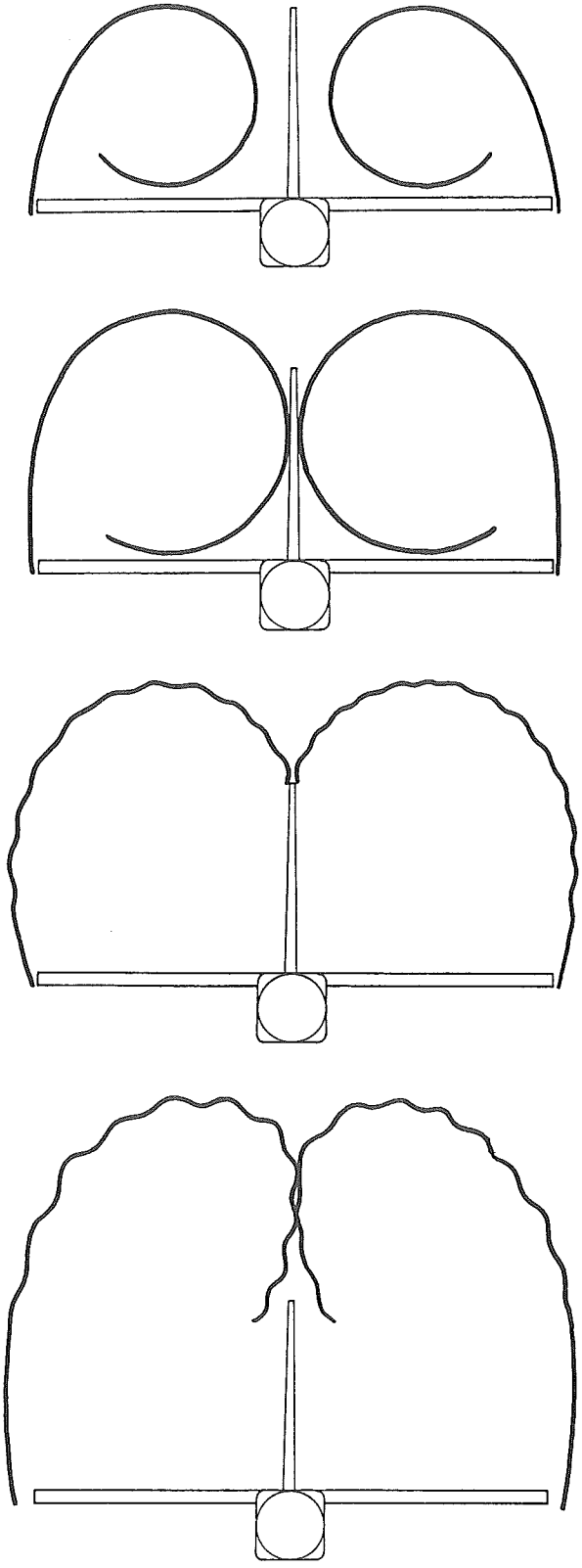

Figure 8: High Wing Flow Visualisation:
a) $\alpha = 36^{\circ}$
b) $\alpha = 40^{\circ}$
c) $\alpha = 44^{\circ}$
d) $\alpha = 58^{\circ}$

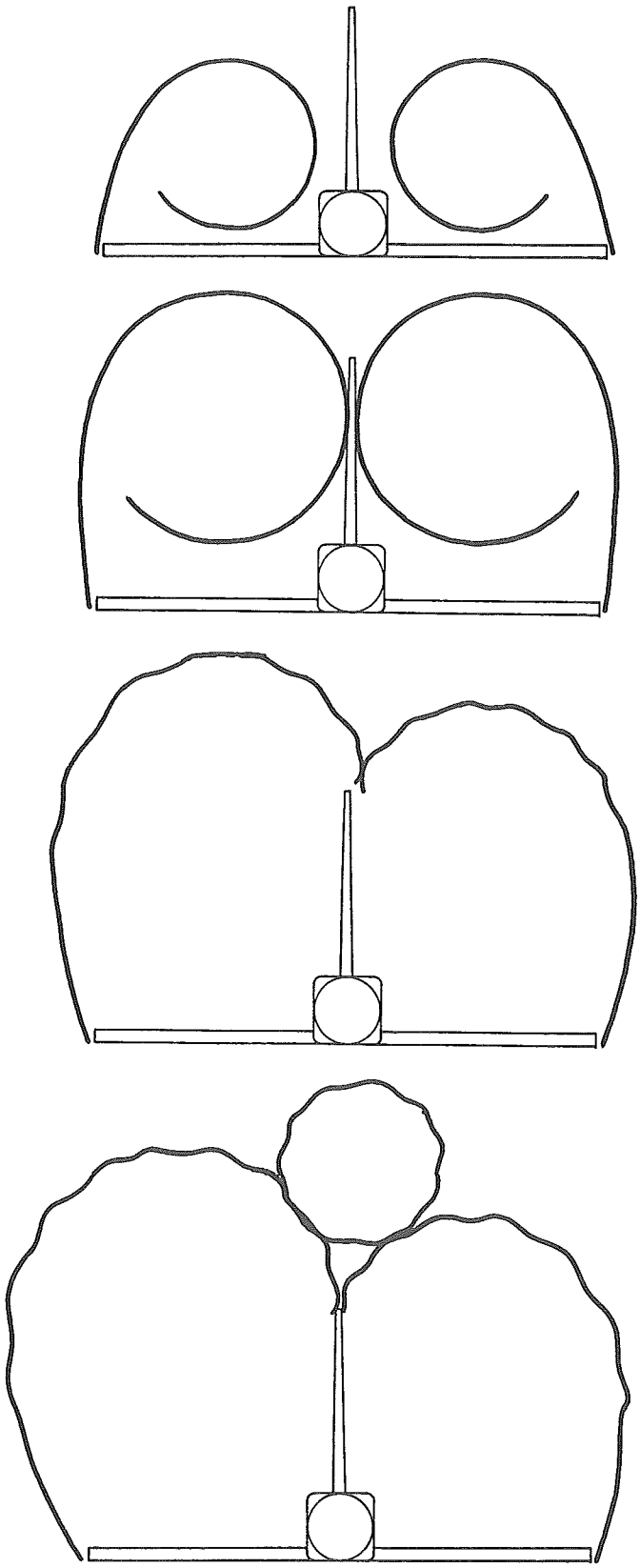

Figure 9: Low Wing Flow Visualisation:
a) $\alpha = 36^{\circ}$
b) $\alpha = 42^{\circ}$
c) $\alpha = 44^{\circ}$
d) $\alpha = 58^{\circ}$

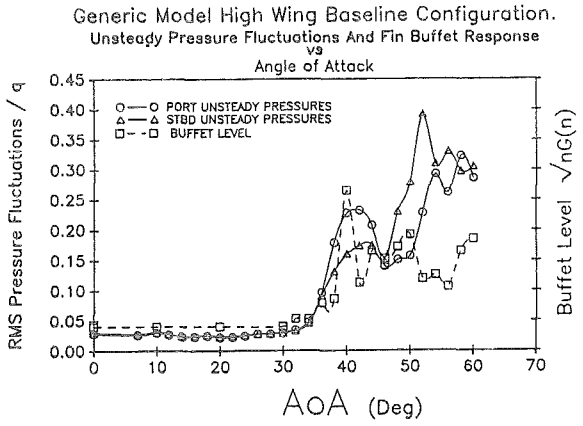

Figure 10: RMS Pressure Fluctuations And Fin Buffet Response vs Angle Of Attack For The High Wing Configuration.

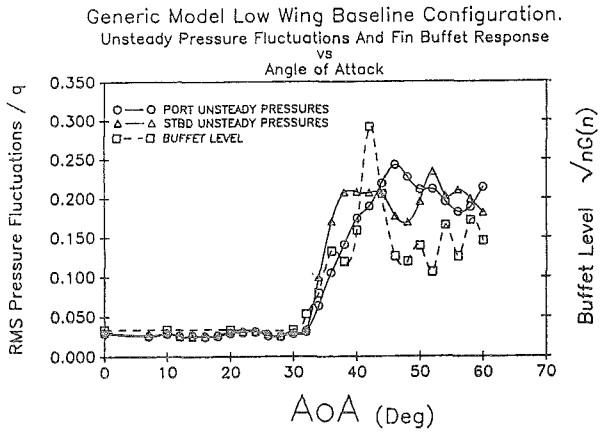

Figure 11: RMS Pressure Fluctuations And Fin Buffet Response vs Angle Of Attack For The Low Wing Configuration.

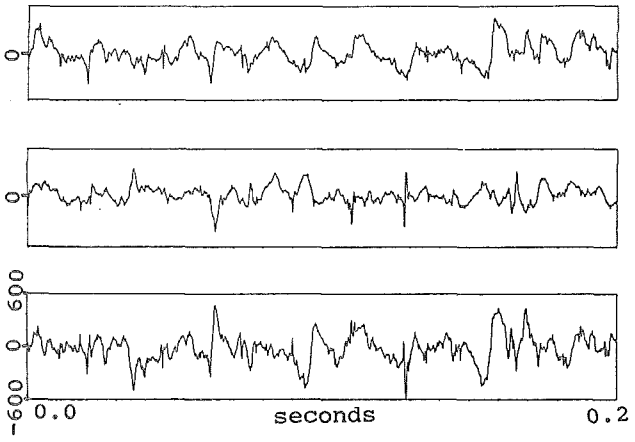

Figure 12: Unsteady Pressure Signals For The High Wing Configuration at α=40°:
a) Port Signal.
b) Starboard Signal.
c) Difference Signal (Port - Stbd).

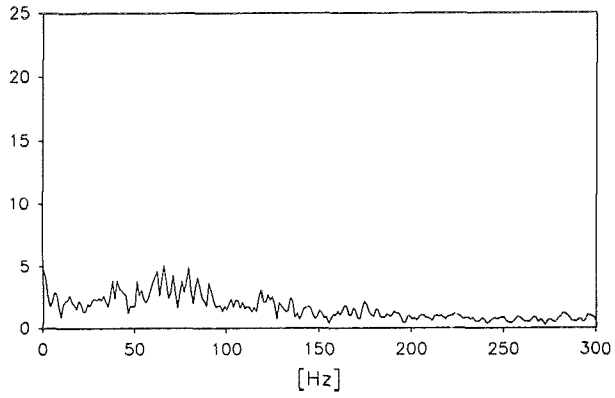

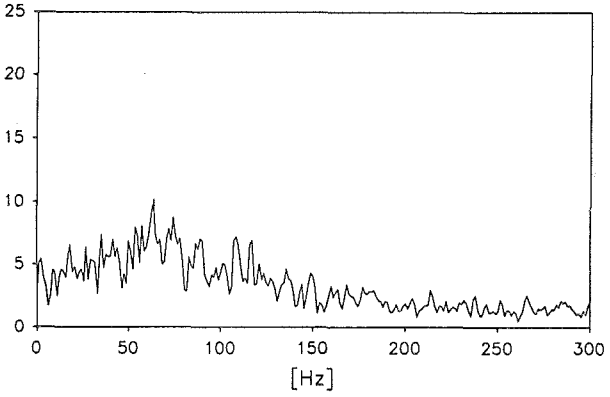

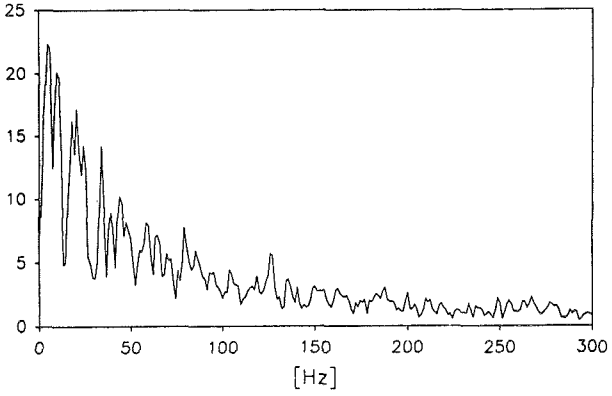

Figure 13: Power Spectral Densities For The High Wing Configuration:
a) α = 36°
b) α = 40°
c) α = 58°

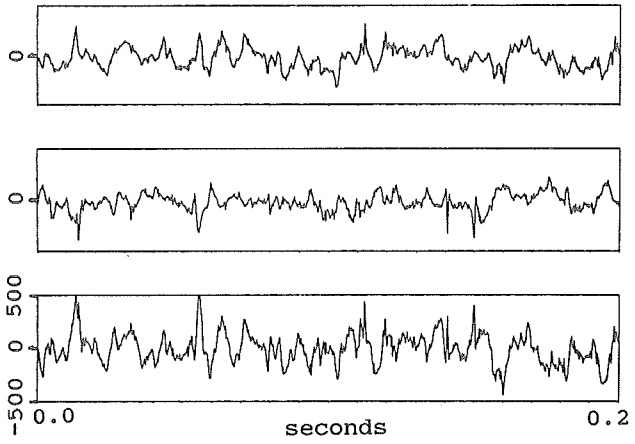

Figure 14: Unsteady Pressure Signals For The Low Wing Configuration At α=42°:
a) Port Signal.
b) Starboard Signal.
c) Difference Signal (Port - Stbd).

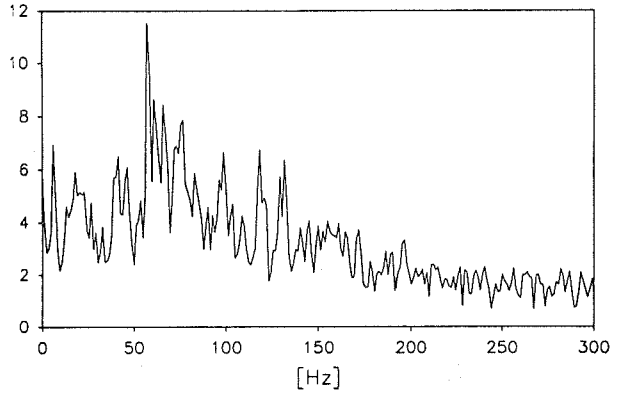

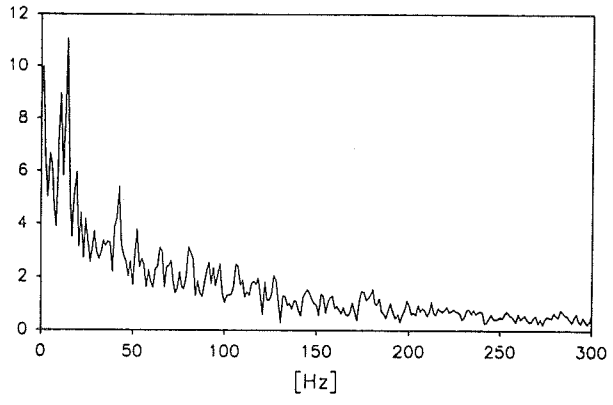

Figure 15: Power Spectral Densities For The Low Wing Configuration:
a) α = 42°
b) α = 58°